Multiple beam splitter using volumetric multiplexed Fresnel zone plates fabricated by ultrafast laser-writing

Jiyeon Choi,[1,2] Mark Ramme,[1] and Martin Richardson[1,*]

[1]*Townes Laser Institute, College of Optics and Photonics, University of Central Florida, 4000 Central Florida Blvd. Orlando, Florida 32816-2700, USA*

[2]*Currently with the Korea Institute of Machinery & Materials, 104 Sinseongno, Yuseong-Gu, Daejeon 305-343, South Korea*

**Corresponding author: mcr@creol.ucf.edu*

Received April 3, 2012; revised July 5, 2012; accepted July 10, 2012; posted July 10, 2012 (Doc. ID 165989); published August 7, 2012

A simple approach to producing a $1 \times N$ beam splitter is demonstrated by fabricating a volumetric multiplex phase Fresnel zone plate in bulk transparent material. This comprised four layers of zone plates created in borosilicate glass by femtosecond laser direct-writing, each shifted laterally relative to the illumination axis, creating four separate beamlets. Since the power transmitted in each beamlet is proportional to the diffraction efficiency of the corresponding zone plate, the power ratios can be customized by adjusting the fabrication parameters of each layer. This approach demonstrates the potential of femtosecond laser direct-writing for the fabrication of complex optical elements in transparent media as components of integrated monolithic photonic devices.

OCIS codes: 050.1965, 140.3390, 350.3950.

Recent trends in microphotonic device manufacturing must satisfy the industry's requirements for compactness, speed, and portability. Fresnel zone plates (FZPs) are attractive as optical elements in these devices, comparing favorably to refractive lens structures due to their thin, planar shape without abandoning functionality. Microimaging systems, optical micro-electro-mechanical systems (MEMS), microsensors and photonic circuits are all possible applications that can benefit from using FZPs [1–4]. Three-dimensional (3D) volumetric phase FZPs provide flexibility for higher-order integration in novel concepts for micro devices. Fabricating these devices by photolithography is constrained by its inherent two-dimensional, layer-by-layer approach. While it is well-suited to mass production, fabricating complex 3D optical structures is limited by mask-fabrication and materials deposition complexities, and ultimately cost considerations. Femtosecond laser direct-writing (FLDW) methods, though less mature, lend themselves to constructing complex 3D optical structures in transparent media in a seamless continuous process, albeit on a sequential unit-fabrication basis. It is therefore more suitable to design-specific 3D photonic devices [5]. Embedded 3D structures are generated by photo-induced localized refractive index change, becoming the building blocks for photonic devices such as waveguides and diffractive optical elements (DOEs) [6,7]. Photo-induced refractive index changes (Δn) can be positive or negative depending on the photo-inducing process and the material selected, and their value is a function of laser dose (energy/unit area). For instance, fused silica and As_2S_3 show positive Δn after laser irradiation, while sodium aluminum phosphate glass and $Ge_{23}Sb_7S_{70}$ exhibit negative Δn [8–11]. For optical guiding structures such as waveguides, a positive Δn is preferred to confine light propagation. Optically diffractive structures such as FZPs, gratings, and other metaoptical elements can utilize positive or negative Δn. This opens a wide range of possible materials for these structures, enabling devices operating from the UV to the mid-IR. We first demonstrated the fabrication of FZP structures in borosilicate glass in 2009 using FLDW [12]. Borosilicate glass has some advantages over fused silica as a material for femtosecond laser-written DOEs, not the least of which is the wider dose range for modified refractive index structures. Early fabrication of FZPs in fused silica relied on laser-induced void generation, rather than refractive index change, resulting in low diffraction efficiencies (2%) [13]. Multiple FZPs in silica were later reported [14,15] using different layer stacking methods to increase the diffraction efficiency. One created an approximation to a four-level zone plate [14], while the other [15] reported a volumetric FZP as a stack of layers, each composed of single tracks as quasi-zones substituting for filled zones. Although these approaches improved the diffraction efficiency η, the slow writing speed required many hours of fabrication time, dimming hopes that this method of FZP production could have practical use. The combined use of fused silica, with its low photosensitivity and small process-window compared to other materials such as chalcogenide and borosilicate glasses, and the consequential need to use amplified low-repetition-rate femtosecond laser systems, impede increasing both processing speed and diffraction efficiency. In the present study, we used borosilicate glass and a femtosecond laser system operating at 200 kHz repetition rate to fabricate multiple arrays of FZPs. This approach overcomes many of the constraints of previous studies. The larger Δn variation with this glass allows us to optimize η. Its higher photosensitivity relative to fused silica reduces the laser dose required, allowing not only for the use of smaller, less complicated, less costly lasers, but also permitting higher processing speeds, with multihundred kilohertz repetition. An additional benefit from operating in this high-repetition rate regime is the higher values of Δn that result from the so-called heat accumulation effect under which the material modification occurs in part through the interaction of the

0146-9592/12/163375-03$15.00/0

laser pulse with material that is at a temperature elevated by the interaction of previous laser pulses. Moreover, we demonstrate for the first time the integration of a multiple FZP array that produces multiple foci with intensity ratios determined by the η of each FZP. This particular structure can be used for applications involving micro-optical devices as integrated optical systems such as spectral splitting or the selection of spectrally coded signals, the multiple coupling of waveguide arrays, or as a substitution for a microlens array. These devices will in the future be used in next-generation communications systems, integrated on-chip sensors and devices, medical inserts and components, and inexpensive single use active detection systems.

In this Letter, we demonstrate the fabrication of a 1×4 beam splitter by constructing a stack of four laser direct-written FZPs spatially separated in a so-called volumetric multiplex FZP. The beam distribution and the diffraction efficiency of the volumetric multiplex FZP are measured. In many cases, a single incident beam needs to be divided into multiple outputs for multichannel coupling to generate duplicated signals or images for multiplexing. Two configurations are possible to divide an incident beam. Figure 1(a) illustrates beam fragmentation using optical means that provide spatial selectivity, while Fig. 1(b) depicts energy attenuation using a partial reflector or a beam splitter. In the former case, the fragments do not retain the profile of the entire input beam. A microlens array is an example of this case. The concept is useful for simple power division or the analysis of wave-front distortion such as in a Shack–Hartmann wave-front sensor. In Fig. 1(b), the divided beams are duplicates of the incident beam guaranteeing the same beam profile. The output beams have the same energy distribution but a weaker intensity corresponding to rI, where r and I are the reflection coefficient of the partial mirror and input intensity, respectively. This type of beam division can also be achieved with a diffractive optical microlens array, such as a 3D multiplex FZP.

In this approach, each layer acts as a lens and a power attenuator. Moreover, the attenuation ratio of each layer can be adjusted precisely by controlling the value of η of each layer, which is easily achievable with FLDW by varying fabrication parameters such as the laser power and writing speed [16]. In our case, r is therefore substituted by η for a single FZP layer, which is determined by the photo-induced phase shift $\Delta\phi$ proportional to both Δn and the modification depth l. Figure 2(a) depicts the concept of a diffractive optical (micro) lens array, implemented by the fabrication of a multiplex FZP consisting of four layers of individual 3D FZPs, each of diameter D with a lateral spacing s. To minimize coupling losses and distortion of the input beam profile, $s \ll D$ should be satisfied; likewise $l < d$ is desirable to avoid the overlap between layers where d is the separation of each FZP.

By keeping the focal length of the top layer f, and that of the nth layer, equal to $f_n = f - nd$, then the focal positions of each FZP are located in the same plane. Alternatively the focal plane of all the separate foci of the individual FZPs can be designed to be in a curved or staggered plane. The intensity of the beam incident on the nth layer can be determined from that on the $(n-1)$th layer as $I_n = (1 - \eta_{n-1})I_{n-1}$, where I_n and η_n are the intensity and diffraction efficiency of the nth FZP, respectively. To fabricate these integrated volumetric diffractive structures in borosilicate glass, we used a Yb-doped fiber-based chirped pulse amplification laser system providing ultrashort pulses with 450 fs duration at a center wavelength of 1043 nm [16]. The computer-controlled direct femtosecond laser-writing station comprised a precision (50 nm) 3D translation stage, together with an in-line high-resolution CCD imaging system. A microscope objective lens (NA = 0.15) was used to focus the 1.25 μJ femtosecond pulses inside the glass, resulting in Δn being $\leq 2 \times 10^{-3}$. The intensity threshold for the refractive index change was measured below 2.4 TW/cm^2 (≤ 0.9 μJ). The modification line width was ~ 5 μm. The 200 kHz repetition rate was chosen to ensure high η from a single FZP by introducing a controlled amount of heat accumulation for the maximum modification l to be ~ 100 μm [16,17]. Figure 2(b) shows a differential interference contrast (DIC) optical microscope image of a laser-written multiplex FZP consisting of four FZP layers fabricated as a 1×4 beam splitter in 1.1 mm thick borosilicate glass. Each FZP, separated from one another by $s = 50$ μm, was created with a zone diameter of 1.1 mm, chosen to be larger than the beam size of the probe laser. The first FZP had a focal length $f_1 = 20$ mm in air, and the focal lengths of the second, third, fourth FZPs were adjusted slightly so that all their foci lay in a common focal plane. The spacing d was 0.15 mm in the medium so that the individual layers did not overlap one another. In designing the individual FZPs, we utilized the central ring method, replacing the normal full zone with a single track. Although this design meant that each FZP had a lower η, for this demonstration it ensured that η was the same for all four layers. It was also assumed that the primary focus distribution of the nth FZP resulted only from diffraction from that layer, without any contributions

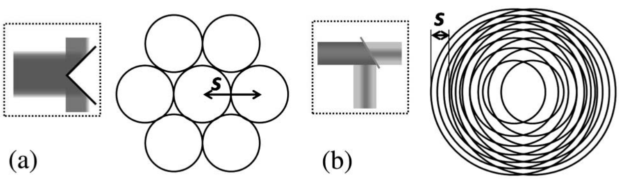

Fig. 1. Beam separation by (a) fragmentation and (b) energy attenuation and corresponding microlens arrays representing similar function.

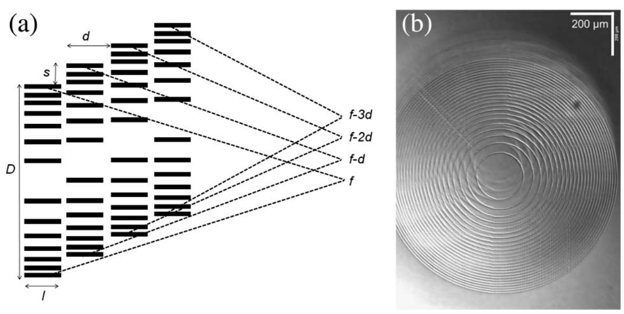

Fig. 2. (a) Schematic diagram of a four-layer multiplex FZP, (b) an optical micrograph of a multiplex FZP, consisting of four FZP layers with the modification depth of ~ 100 μm, written in a piece of borosilicate glass.

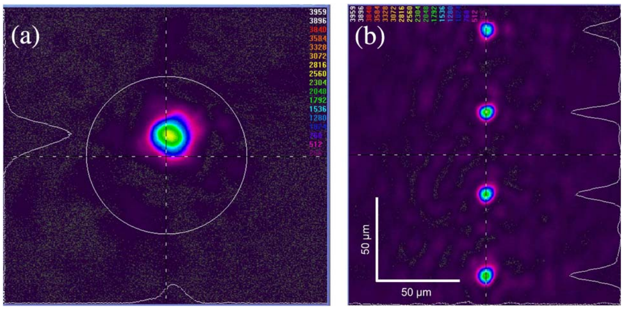

Fig. 3. (Color online) Intensity profile of (a) incident beam, (b) foci from a 1×4 volumetric multiplex FZP.

coming from the other layers. Thus, multiple diffraction that may result in cross-talk between layers was not taken into account. This is reasonable since η for each layer was chosen to be less than 5% in this demonstration. The η of each of the FZPs in the integrated structure was examined with 543.5 nm light from an HeNe laser. The incident power of the probe beam on the FZP was 240 μW; the beam diameter $2\omega_o$ was measured to be $\sim$0.95 mm using a knife edge method. The diffracted beam profiles and η were measured with a CCD beam profiler and a power meter, respectively. An imaging system was employed between the sample and the detector. An iris was inserted behind the FZP to block the undiffracted beam. Figures 3(a) and 3(b) are images of the incident beam and the four focused beams through the multiplexed FZP structure. As seen in Fig. 3(b), the intensity distribution of four foci shows equally distributed intensities. The measured intensity ratios of the primary foci $f_1 : f_2 : f_3 : f_4$ are $1 : 0.94 : 0.85 : 0.82$ from the bottom focus distribution to the top focus. The individual diffraction efficiencies $\eta_1 : \eta_2 : \eta_3 : \eta_4$ were measured to be 3.1%, 3.0%, 2.8%, and 2.7%, respectively. The total η was estimated to be $\sim$11.5%. The spacing between foci is about the same as prescribed by the original design; that is $s = 50\ \mu$m.

It is seen that the η slightly decreases from 3.1% to 2.7% from the first to the fourth (deepest) layer, and that there is a decrease for deeper layers. This implies that the effective writing intensity might gradually decrease with depth, even though the writing parameters were kept identical for each FZP layer. This is probably due to the nonlinear optical effect of the medium affecting the focusing geometry at deeper locations. One can readily compensate for this by adjusting the laser power as a function of depth of the FZP layer being written. More interestingly, one can design arbitrary combination of FZPs to customize their η ratios and their working wavelengths by changing the fabrication parameters to produce any desired intensity ratio at the focal plane. This is promising for some applications such as soliton propagation or spectral beam splitting. One can develop a simple coupling optics for the irradiation of waveguide arrays with different input powers and wavelengths, with controlled coupling efficiency for each waveguide. A simple extension of this technology would be the addition of an optically pumped microfluidic reservoir associated with an array of customized FZPs that act as spectral filters for fluorescence measurements of complex chemicals.

References

1. S. Sinzinger and J. Jahns, Appl. Opt. **36**, 4729 (1997).
2. Y. Wang, W. Yun, and C. Jacobsen, Nature **424**, 50 (2003).
3. K. Hedsten, J. Melin, J. Bengtsson, P. Modh, D. Karln, B. Lfving, R. Nilsson, H. Rdjegrd, K. Persson, and P. Enoksson, Sens. Actuators A **142**, 336 (2008).
4. J. Fonollosa, R. Rubio, S. Hartwig, S. Marco, J. Santander, L. Fonseca, J. Wöllenstein, and M. Moreno, Sens. Actuators A **132**, 498 (2008).
5. R. R. Gattass and E. Mazur, Nature Photon **2**, 219 (2008).
6. A. M. Streltsov and N. F. Borrelli, Opt. Lett. **26**, 42 (2001).
7. G. D. Marshall, M. Ams, and M. J. Withford, Opt. Lett. **31**, 2690 (2006).
8. K. Miura, J. Qiu, H. Inouye, T. Mitsuyu, and K. Hirao, Appl. Phys. Lett. **71**, 3329 (1997).
9. T. Anderson, L. Petit, N. Carlie, J. Choi, J. Hu, A. M. Agarwal, L. C. Kimerling, K. Richardson, and M. Richardson, Opt. Express **16**, 20081 (2008).
10. A. Zoubir, M. Richardson, C. Rivero, A. Schulte, C. Lopez, K. Richardson, N. Ho, and R. Vallée, Opt. Lett. **29**, 748 (2004).
11. J. W. Chan, T. R. Huser, S. H. Risbud, J. S. Hayden, and D. M. Krol, Appl. Phys. Lett. **82**, 2371 (2003).
12. J. Choi and M. Richardson, Proc. SPIE **7203**, 72030G (2009).
13. W. Watababe, D. Kuroda, K. Itoh, and J. Nishii, Opt. Express **10**, 978 (2002).
14. K. Yamada, W. Watanabe, Y. Li, K. Itoh, and J. Nishii, Opt. Lett. **29**, 1846 (2004).
15. P. Srisungsitthisunti, O. K. Ersoy, and X. Xu, Appl. Phys. Lett. **90**, 011104 (2007).
16. J. Choi, M. Ramme, T. Anderson, and M. Richardson, Proc. SPIE **7589**, 7589-44 (2010).
17. M. Shimizu, M. Sakakura, M. Ohnishi, Y. Shimotsuma, T. Nakaya, K. Miura, and K. Hirao, J. Appl. Phys. **108**, 073533 (2010).